Finite Amplitude Waves in Stratified Two-Phase Flow: Transition to Slug Flow

In horizontal two-phase flow, transition from stratified to slug flow occurs due to the nonlinear instability of finite amplitude interfacial waves. The nonlinear equations describing interfacial waves in stratified two-phase flow are solved by a multiple scales perturbation method. Instability criteria and amplification factors are determined. The phase velocities that are calculated to lead to amplification of finite amplitude interfacial waves are well below those based on linear stability criteria. This is in agreement with existing experimental data on transition from stratified to slug flow in horizontal channels.

RAFI AHMED
and SANJOY BANERJEE

University of California
Santa Barbara, CA 93106

SCOPE

Multiphase flows are of importance in a variety of industrial and geophysical processes. Since the underlying mechanisms governing interfacial transport are complex, prediction of two-phase parameters from first principles is extremely difficult. In particular, it has been observed that transport processes change qualitatively when interfacial configuration changes. Therefore, transitions between flow regimes have been studied intensively, but the mechanisms are not fully understood.

In horizontal two-phase flow, phases stratify due to density differences if the velocity difference between the phases is small relative to the phase velocities. As the velocity difference between the phases is increased, waves appear on the initially smooth interface but the phases remain distinctly separated. At sufficiently high velocity differences interfacial waves grow rapidly, tending to block the flow, i.e., they are swept up to form slugs. This transition takes place when the flow conditions are such that initially small but finite-amplitude waves become unstable and undergo unbounded growth.

Theoretical work on transition to slug flow has not yet led to an understanding of why the transition occurs at phase velocity differences below that required for the linear Kelvin-Helmholtz instability, although this has been observed in experiments. To get some insight into this phenomenon we investigated the growth of nonlinear finite amplitude interfacial waves.

The objective of this study is to analytically establish a criterion for nonlinear instability of the finite amplitude waves on the interface of two bounded fluids. This criterion is then to be applied to interpreting experiments on the transition from stratified to slug flow.

CONCLUSIONS AND SIGNIFICANCE

A perturbation technique based on the method of multiple scales is used here to solve the system of equations governing finite amplitude waves at the interface between two bounded fluids. This method allows us to separate the system into two parts: the rapidly varying phase of the disturbances, and the slowly varying amplitude. It is found that the complex system of equations governing the modulation of the wave amplitude can be reduced to a nonlinear Schrodinger equation. Nonlinear instability is shown to be essentially determined by the signs of two coefficients in the Schrodinger equation, leading to an analytically established criterion for the growth of finite-amplitude waves at the interface between two bounded flowing fluids. The predictions made by this study are in reasonable agreement with existing experimental results and appear to provide a theoretical framework for interpreting experiments on transition from stratified to slug flow. It is evident from the calculations of critical air velocity that nonlinearity has a destabilizing effect in this case; this study, therefore, provides an explanation as to why instability occurs in experiments well below the critical velocities predicted by linear analysis.

INTRODUCTION

Theoretical work on transition to slug flow has not led to an understanding of why transition occurs at relative velocities below that required for linear Kelvin-Helmholtz instability, although this has been observed in experiments.

For example, Wallis and Dobson (1973) have published experimental results for transition from wavy to slug flow in a horizontal

rectangular duct. It was found that transition occurred at relative velocities well below the threshold values for the linear Kelvin-Helmholtz instability. They proposed a semiempirical criterion for this transition. This criterion was in good agreement with their experimental results, however it did not have a theoretical basis. Taitel and Dukler (1976) proposed a criterion similar to that of Wallis and Dobson, but in their case one of the coefficients was replaced by the void fraction in the duct. They also found that their correlation was in fairly good agreement with the slug formation experiments done by Kordyban and Ranov (1970).

Theoretical work somewhat related to the problem we are discussing here has been reported by several investigators. For a layer of arbitrary depth, Whitham (1967) and Benjamin (1967), using different methods, showed that the nonlinear modulation in wave trains is stable or unstable according as $kh <$ or > 1.363. Hasimoto and Ono (1972) derived a nonlinear Schrodinger equation for the modulation of waves on the surface of a bounded liquid layer by using the method of multiple scales. By a stability analysis of the governing Schrodinger equation, they arrived at the Whitham-Benjamin criterion for instability. This result was also experimentally observed by Benjamin and Feir (1967).

The experimental results of Lake and Yuen (1977) for unbounded fluids suggest that wind waves under steady wind conditions have properties very similar to the nonlinear Stokes wave train. Stuart and DiPrima (1978) showed that wind waves governed by the Schrodinger equation are also similar to the Stokes wave train with nonlinear effects leading to sideband instabilities and breakup of the wave trains. Weissman (1978) investigated the nonlinear Kelvin-Helmholtz instability of unbounded fluids in relative motion. He showed that the derivation of amplitude equations, first-order and second-order in time, depends upon the linear dispersion relation used, which is different for stable and marginally unstable modes. In that study the principal concern was the nonlinear development of disturbances in the neighborhood of the marginal curve.

As is evident from the foregoing review, the nonlinear interfacial instability between two bounded and flowing fluids has not yet been investigated, nor has any explicit criterion been proposed for such an instability. This study, therefore, analytically investigates nonlinear instability of finite-amplitude waves on the interface between two bounded fluids.

PROBLEM FORMULATION

Nonlinear dispersive waves are investigated here at the interface of two fluids of arbitrary depths in a horizontal rectangular duct.

A Cartesian coordinate system is introduced such that the x-axis lies in the undisturbed fluid interface, while the y-axis is normal to the interface. The wave train is assumed to be propagating in the positive x direction, whereas the body force is acting in the negative y direction, as shown in Figure 1. Fluids in both phases are moving with uniform velocities parallel to the interface The density of the lower phase is taken to be greater than that of the upper phase.

Since we are mostly interested in the gas-water system at low Mach numbers, we assume the fluids to be incompressible. In this paper we also neglect boundary layer effects and confine the problem to inviscid flow. This assumption is rather artificial and eliminates dynamic instabilities that may arise out of viscous effects; it is an aspect that will be considered in a later paper. The initial motions of the fluids are also assumed to be irrotational and thus can be represented by potential functions. Dimensionless quantities are introduced using the characteristic length $l = (h + \tilde{h})$ and characteristic time $(l/g)^{1/2}$.

The velocity potentials of the perturbed and total motion of the fluids in their respective phases (Figure 1) are related by the following equations:

$$\Phi = \varphi + vx \tag{1}$$

$$\tilde{\Phi} = \tilde{\varphi} + \tilde{v}x \tag{2}$$

Then wave propagation is governed by the Laplace Eqns. 3 and 4, subject to the boundary conditions of Eqs. (5–9) for inviscid flow:

$$\nabla^2\Phi = 0 \tag{3}$$

$$\nabla^2\tilde{\Phi} = 0 \tag{4}$$

$$\frac{\partial\Phi}{\partial y} = 0 \tag{5}$$

$$\text{at } y = -h$$

$$\frac{\partial\tilde{\Phi}}{\partial y} = 0 \tag{6}$$

$$\text{at } y = +\tilde{h}$$

The kinematic conditions at the interface are given by the following equations:

$$\frac{\partial\Phi}{\partial y} = \frac{\partial\eta}{\partial t} + \frac{\partial\Phi}{\partial x}\frac{\partial\eta}{\partial x} \quad \text{at } y = \eta(x,t) \tag{7}$$

$$\frac{\partial\tilde{\Phi}}{\partial y} = \frac{\partial\eta}{\partial t} + \frac{\partial\tilde{\Phi}}{\partial x}\frac{\partial\eta}{\partial x} \quad \text{at } y = \eta(x,t) \tag{8}$$

The dynamic boundary condition at the interface is given by

$$\eta = -\frac{1}{G}\left(\frac{\partial\Phi}{\partial t} + \frac{1}{2}(\tilde{\nabla}\Phi)^2\right) + \frac{\rho'}{G}\left(\frac{\partial\tilde{\Phi}}{\partial t} + \frac{1}{2}(\tilde{\nabla}\tilde{\Phi})^2\right) \tag{9}$$

$$\text{at } y = \eta(x,t)$$

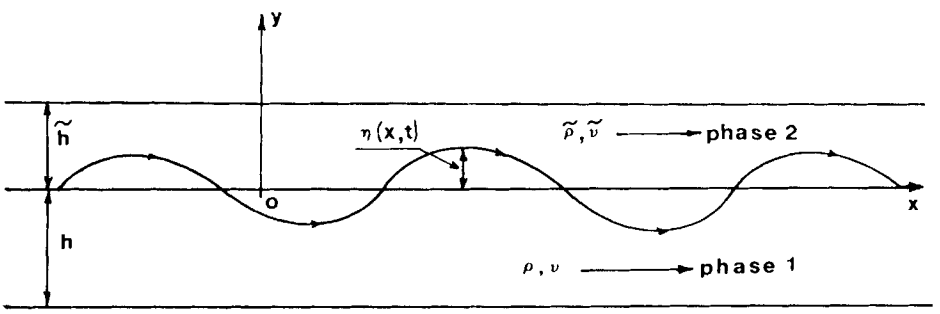

Figure 1. Schematic diagram of stratified flow defining symbols.

For viscous flows, continuity of tangential velocity and stress would be additional boundary conditions required at the interface.

We have three interfacial boundary conditions. However we can eliminate η from first order terms in Eqs. 7 and 8 by making use of Eq. 9 and thereby reduce them to two. We determine $\partial\eta/\partial t$ and $\partial\eta/\partial x$ from Eq. 9 and substitute them in Eqs. 7 and 8. These equations are given by:

$$\varphi_y = -\frac{1}{G}[\varphi_{tt} + 2(\varphi_x + v)\varphi_{xt} + \varphi_y\varphi_{yt} + (\varphi_x + v)^2\varphi_{xx} + \varphi_y\varphi_{xy}(\varphi_x + v)] + \frac{\rho'}{G}[\tilde{\varphi}_{tt}\{\tilde{\varphi}_{xt} + (\tilde{\varphi}_x + \tilde{v})\tilde{\varphi}_{xx} + \tilde{\varphi}_y\tilde{\varphi}_{xy}\}(\varphi_x + v) + \tilde{\varphi}_y\tilde{\varphi}_{yt} + \tilde{\varphi}_{xt}(\tilde{\varphi}_x + \tilde{v})] \quad (10)$$

$$\text{at } y = \eta(x,t)$$

$$\tilde{\varphi}_y = -\frac{1}{G}[\varphi_{tt} + \varphi_{xt}(\varphi_x + v) + \varphi_y\varphi_{yt} + (\tilde{\varphi}_x + \tilde{v}) \times \{\varphi_{xt} + \varphi_{xx}(\varphi_x + v) + ph_y\varphi_{xy}\}] + \frac{\rho'}{G}[\tilde{\varphi}_{tt} + 2(\tilde{\varphi}_x + \tilde{v})\tilde{\varphi}_{xt} + \tilde{\varphi}_{xx}(\tilde{\varphi}_x + \tilde{v})^2 + \tilde{\varphi}_y\tilde{\varphi}_{yt} + \tilde{\varphi}_y\tilde{\varphi}_{xy}(\tilde{\varphi}_x + \tilde{v})] \quad (11)$$

$$\text{at } y = \eta(x,t)$$

Here subscripts denote partial differentiation with respect to itself.

Solution of the Laplacian Expression in the Differential Operator Form

If the solution of Eqs. (3) and (4) satisfying the boundary conditions of Eqs. 5 and 6 can be incorporated in Eqs. 10, 11, and 9, then these equations become the governing equations of the problem.

The solution of Eq. 3 satisfying the boundary condition in Eq. 5 in the operator form is given by

$$\varphi(x,y,t) = \frac{\cosh(p(y+h))}{\cosh(ph)} f(x,t) = \left(1 + ypT + \frac{y^2p^2}{2!} + \frac{Ty^3p^3}{3!} + O(y^4)\right) f(x,t) \quad (12)$$

Similarly, the solution of Eq. 4 satisfying the boundary condition in Eq. 6 can be written in the operator form as

$$\tilde{\varphi}(x,y,t) = \frac{\cosh(p(y-\tilde{h}))}{\cosh(p\tilde{})} \tilde{f}(x,t) = \left(1 - yp\tilde{T} + \frac{y^2p^2}{2!} - \frac{\tilde{T}y^3p^3}{3!} + O(y^4)\right) \tilde{f}(x,t) \quad (13)$$

Here f and $\tilde{f}$ are periodic functions in x and t.

The derivation of these equations is given in the Supplement to this paper.

Substituting Eqs. 12 and 13 into Eqs. 10, 11, and 9, and retaining only second order terms in $\eta(x,t)$, these equations can be written in the differential operator form. These equations are given in the Supplement to this paper.

METHOD OF SOLUTION

To investigate the modulation of nonlinear interfacial waves we use a perturbation technique based on the method of multiple scales (see for example Whitham, 1974, and Nayfeh, 1973). When wave amplitude is small but finite, the nonlinear terms give rise to a slow modulation of amplitude. The method of multiple scales allows us to separate the system into a rapidly varying part—phase—governed by fast scales and a slowly varying part—amplitude—governed by slow scales.

Perturbation Scheme

In order to determine a uniformly valid perturbation solution of the governing equations we use the variables of multiple scales defined as follows: $t = t; t_1 = \epsilon t; t_2 = \epsilon^2 t; x = x; x_1 = \epsilon x$, where ϵ is a small dimensionless parameter, usually of the order of the maximum steepness of the wave.

We seek the solution in the form of asymptotically expanded series:

$$f(x,t) = \sum_{n=1}^{3} \epsilon^n f_n(x,x_1,t,t_1,t_2) + O(\epsilon^4)$$
$$\tilde{f}(x,t) = \sum_{n=1}^{3} \epsilon^n \tilde{f}_n(x,x_1,t,t_1,t_2) + O(\epsilon^4) \quad (14)$$
$$\eta = \sum_{n=1}^{2} \epsilon^n \eta_n(x,x_1,t,t_1,t_2) + O(\epsilon^3)$$

Since the number of variables has been increased, the time derivatives and space derivatives are transformed by using the following chain rules:

$$q = q + \epsilon q_1 + \epsilon^2 q_2$$
$$q^2 = q^2 + 2\epsilon q q_1 + \epsilon^2(2qq_2 + q_1^2) \quad (15)$$
$$p^2 = p^2 + 2\epsilon p p_1 + \epsilon^2 p_1^2$$
$$pT = pT + \epsilon(pt)'p_1 + \frac{1}{2}\epsilon^2(pT)_1^2$$

where prime $'$ denotes derivative with respect to p and

$$p_1 = -i\frac{\partial}{\partial x_1}, \quad q_1 = i\frac{\partial}{\partial t_1}, \quad q_2 = i\frac{\partial}{\partial t_2} \quad (16)$$

Substituting Eq. 15 and making use of Eq. 16 in the governing equations, and equating the coefficients of like powers of ϵ, we get equations of different orders of ϵ.

These perturbation equations are given in the Supplement.

Solutions of the First-Order Equations

The first-order equations are a pair of coupled linear equations. They can be written in the following form:

$$\boldsymbol{D}\boldsymbol{F}_1 = 0 \quad (17)$$

where the operator matrix $\boldsymbol{D}$ is defined by

$$\boldsymbol{D} = \begin{bmatrix} GpT + (2vqp - q^2 - v^2p^2) & (v+\tilde{v})qp - v\tilde{v}p^2 - q^2 \\ \rho'(q^2 + v\tilde{v}p^2 - (v+v)qp) & \rho'(\tilde{v}^2p^2 + q2 - 2\tilde{v}qp) - Gp\tilde{T} \end{bmatrix} \quad (18)$$

and the column vector

$$\boldsymbol{F}_1 = \begin{bmatrix} f_1(x,t) \\ \tilde{f}_1(x,t) \end{bmatrix} \quad (19)$$

The solutions of Eq. 19 are given by Eqs. 20 and 21 subject to a solvability condition, Eq. 24. The solutions are:

$$f_1 = AL\exp[i\vartheta] + cc + C \quad (20)$$
$$\tilde{f}_1 = A\tilde{L}\exp[i\vartheta] + cc + \tilde{C} \quad (21)$$

where $\vartheta = kx - \omega t$ and A, C, and $\tilde{C}$ are functions of slow variables x_1, t_1, and t_2 and

$$L = -\frac{(w - vk)}{\sigma} \quad (22)$$

$$\tilde{L} = \frac{(w - \tilde{k})}{\tilde{\sigma}} \tag{23}$$

The solvability condition for the nontrivial solution of Eq. 17 yields

$$\omega = \frac{k(v\tilde{\sigma} + \rho'\tilde{v}\sigma) \pm [\sigma\tilde{\sigma}(Gk(\tilde{\sigma} + \rho'\sigma) - \rho'(v - \tilde{v})^2k^2)]^{1/2}}{(\tilde{\sigma} + \rho'\sigma)} \tag{24}$$

Equation 24 gives the dispersion relation.

In Eq. 24, for real values of ω the following condition must be satisfied:

$$G(\tilde{\sigma} + \rho'\sigma) - k\rho'(v - \tilde{v})^2 \geq 0 \tag{25}$$

If the above condition is not satisfied, this gives rise to linear Kelvin-Helmholtz instability.

Now substituting the values f_1 and $\tilde{f}_1$ in the following first-order equation

$$\eta_1 = i\frac{\rho'}{G}[\tilde{v}pf_1 - q\tilde{f}_1] - \frac{i}{G}[vpf_1 - qf_1] \tag{26}$$

we get

$$\eta_1 = -ikAe^{i\vartheta} + cc \tag{27}$$

Equation 27 gives the wave profile to the first-order approximation; However, $A(x_1,t_1,t_2)$ is undermined at this stage.

Second-Order Equations

Substituting the values of f_1, $\tilde{f}_1$ and η_1 in the second-order equations, we arrive at second-order linear equations whose inhomogeneous parts are known. This is given by

$$\boldsymbol{D}\boldsymbol{F}_2 = \boldsymbol{I}_1 \tag{28}$$

where the column vectors are defined as

$$\boldsymbol{F}_2 = \begin{pmatrix} f_2 \\ \tilde{f}_2 \end{pmatrix} \tag{29}$$

and

$$\boldsymbol{I}_1 = \begin{bmatrix} RA^2e^{2i\vartheta} + Se^{i\vartheta} + cc \\ \tilde{R}A^2e^{2i\vartheta} + \tilde{S}e^{i\vartheta} + cc \end{bmatrix} \tag{30}$$

where R, $\tilde{R}$, S, and $\tilde{S}$ are given in the Supplement.

We have seen in the previous section that the homogeneous solutions of Eq. 28 have terms proportional to $\exp[\pm i\vartheta]$. Therefore, the inhomogeneous part of the equation containing terms proportional to $\exp[\pm i\vartheta]$ will produce secular terms in the solutions of $\boldsymbol{F}_2$; that is, its particular solution will have terms proportional to $(xe^{i\vartheta})$ or $(te^{i\vartheta})$—the so-called secular terms. The condition for a unformly valid perturbation solution requires that the inhomogeneous part of the equation be orthogonal to every solution of the adjoint homogeneous problem.

Since the operator matrix $\boldsymbol{D}$ is a 2×2 matrix, there are two adjoint homogeneous solutions of Eq. 28, but they can be reduced to one by using the dispersion relation, Eq. 24. This is given by:

$$(q_1A) - V(\omega,k)(p_1A) = 0 \tag{31}$$

where $V(w,k)$ is found to be equal to dw/dk, the group velocity of the waves:

$$\frac{d\omega}{dk} = \frac{G\sigma\tilde{\sigma} + Gk(\sigma\tilde{\sigma}) + 2(v\tilde{\sigma}\omega_1 + \rho'\tilde{v}\sigma\omega_2) - \rho'\sigma'\omega_2^2 - \tilde{\sigma}'\omega_1^2}{2\omega(\tilde{\sigma} + \rho'\sigma) - 2k(v\tilde{\sigma} + \rho'\tilde{v}\sigma)} \tag{32}$$

We introduce a new variable

$$\xi = x_1 - Vt_1 \tag{33}$$

Using this new variable in Eq. 31 we get

$$A(x_1,t_1,t_2) = A(\xi,t_2) \tag{34}$$

The above condition implies that the slow modulation of the wave packet due to weak nonlinearity propagates with the group velocity.

By using the method of undetermined coefficients, we obtain the following particular solutions of the second-order equations:

$$f_2 = iMA^2e^{2i\vartheta} + cc \tag{35}$$

$$\tilde{f}_2 = i\tilde{M}A^2e^{2i\vartheta} + cc \tag{36}$$

Substituting the values of f_1, $\tilde{f}_1$, f_2, $\tilde{f}_2$ and η_1 in the third-order equation we get:

$$\eta_2 = N_1A^2e^{2i\vartheta} + N_2A_\xi e^{i\vartheta} + cc + N_3(A\bar{A}) + N_4C_\xi + \tilde{N}_4\tilde{C}_\xi \tag{37}$$

M, $\tilde{M}$, N_1, N_2, N_3, N_4, and $\tilde{N}_4$ are given in the Supplement.

Third-Order Equations

In order to determine the differential equation which governs the amplitude modulation, we must proceed to the third-order perturbation equations and impose a solvability condition:

$$\boldsymbol{D}\boldsymbol{F}_3 = \boldsymbol{I}_3 + (\boldsymbol{I}_4 - \boldsymbol{I}_5\boldsymbol{I}_6) + NST \tag{38}$$

where

$$\boldsymbol{F}_3 = \begin{pmatrix} f_3 \\ \tilde{f}_3 \end{pmatrix} \tag{39}$$

$$\boldsymbol{I}_3 = \begin{bmatrix} (Q + J + v_2A^2\bar{A})e^{i\vartheta} + cc \\ (\tilde{Q} + \tilde{J} + \tilde{v}_2A^2\bar{A})e^{i\vartheta} + cc \end{bmatrix} \tag{40}$$

$$\boldsymbol{I}_4 = \begin{bmatrix} z(A\bar{A})_\xi e^{in\vartheta} \\ z(A\bar{A})_\xi e^{in\vartheta} \end{bmatrix}_{n=0} \tag{41}$$

$$\boldsymbol{I}_5 = \begin{bmatrix} \frac{G}{2}(pT)''p_1^2 - O_1 & \rho'O_s \\ -O_s & \rho'O_2 - \frac{G}{2}(p\tilde{T})''p_1^2 \end{bmatrix} \tag{42}$$

$$\boldsymbol{I}_6 = \begin{bmatrix} Ce^{in\vartheta} \\ \tilde{C}e^{in\vartheta} \end{bmatrix}_{n=0} \tag{43}$$

NST refers to those terms which do not produce secular terms, namely, the terms of second and third harmonics. $[e^{in\vartheta}]_{n=0}$ refers to the mean harmonic terms. O_1, O_2, O_3, Q, $\tilde{Q}$, J, $\tilde{J}$, v_2, $\tilde{v}_2$, z, and $\tilde{z}$ are given in the Supplement.

Since the homogeneous solutions of the third-order equations have terms proportional to first and mean harmonics—i.e., terms containing $\exp(in\vartheta)$ and $[\exp(in\vartheta)]_{n=0}$—these terms in the inhomogeneous parts of these equations will produce secular terms. To eliminate these secular terms we use the same arguments as we did in the case of the second-order equations and impose a solvability condition. In Eq. 38 we eliminate the secular terms in two stages and finally arrive at the following solvability condition given by:

$$\begin{vmatrix} \rho'\sigma\omega_2 & Q + vA^2\bar{A} \\ \tilde{\sigma}\omega_1 & \tilde{Q} + \tilde{v}A^2\bar{A} \end{vmatrix} = 0 \tag{44}$$

After algebraic manipulation, the above equation simplifies to:

$$\frac{1}{i}\frac{\partial A}{\partial \tau} = \alpha\frac{\partial^2 A}{\partial \xi^2} + \beta A^2\bar{A} \tag{45}$$

This is a Schrodinger equation with a cubic nonlinearity, which governs the slow modulation of the amplitude (Whitham, 1974).

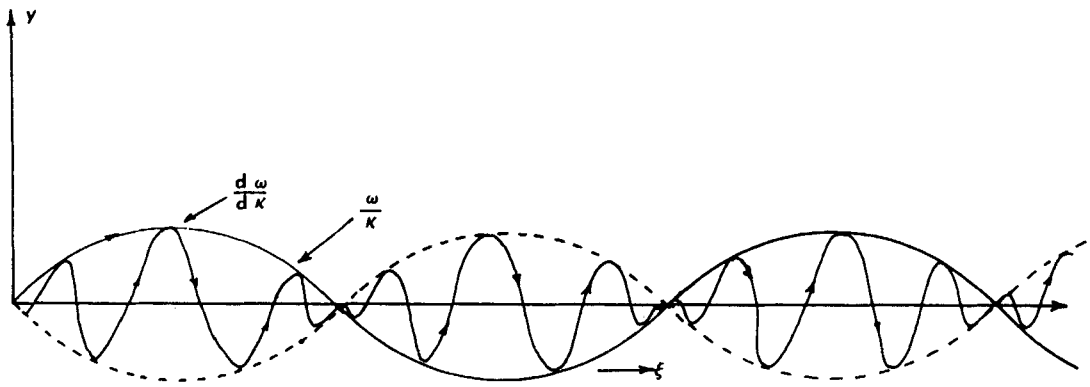

Figure 2. Schematic diagram of wav amplitude and modulation.

In Eq. 45, α and β are functions of ρ', k, h, $\tilde{h}$, v and $\tilde{v}$; they are given by following equations:

$$\beta = \frac{-(\nu\tilde{\sigma}\omega_1 + \rho'\sigma\tilde{v}\omega_2)}{2Gk(\rho'\sigma\omega_2 + \tilde{\sigma}\omega_1)} \tag{46}$$

$$\alpha = \frac{1}{2(\tilde{\sigma}\omega_1 + \rho'\sigma\omega_2)}\left[\frac{1}{k\sigma\tilde{\sigma}}(\rho'\sigma^2\tilde{\sigma}'\omega_2^2 + \tilde{\sigma}^2\sigma'\omega_1^2) + \frac{1}{2\sigma\tilde{\sigma}}(\rho'\sigma^2\tilde{\sigma}''\omega_2^2 + \tilde{\sigma}^2\sigma''\omega_1^2)\right.$$
$$\left.\times\{-\tilde{\sigma}(V-v)^2 + \rho'\sigma(V-\tilde{v})^2\} + \frac{1}{Gk}\{\rho'(\omega_2(V-v) - (V-\tilde{v})\omega_1)^2\}\right] \tag{47}$$

In the single phase when the free stream velocity is zero, the expressions for α and β reduce to Hasimoto and Ono's (1972) μ and ν.

SOLUTION OF THE SCHRODINGER EQUATION

The solution of the Schrodinger equation, Eq. 45, is (Hasimoto and Ono, 1972):

$$A = A_0 \exp[i(\psi\tau - \xi k')] \tag{48}$$

where

$$\psi = -ak'^2 + \beta|A_0|^2 \tag{49}$$

and A_o is a constant.

Derived from the above solution, the envelope of the wave packet, which modulates in both time and space, is schematically shown in Figure 2. In this figure the solid line represents the actual envelope, the dotted line its mirror image, and the arrowhead line the general wave profile.

If in the Eq. 48 solution of the Schrodinger equation k' is put equal to zero—that is, the amplitude is assumed to be modulating only in time—then we have

$$A = A_0 \exp[i\beta|A_0|^2\tau] \tag{50}$$

where A_o is the initial amplitude. This solution represents the uniform wavetrain.

Derivation of Stokes Waves

We can write η, the wave profile, in the following form:

$$\eta = -i\epsilon kAe^{i\vartheta} + \epsilon^2(N1A^2e^{2i\vartheta} + N_2A_\xi e^{i\vartheta}) + cc + \epsilon^2(N_3 + N_4B + \tilde{N}_4\tilde{B})(A\bar{A}) \tag{51}$$

In the uniform wavetrain solution of the Schrodinger equation we set

$$A_o = -\frac{a}{2ik} \tag{52}$$

where a is a real constant.

Substituting this value of A_o in Eq. 51 we get

$$\eta = \epsilon a\cos(\zeta) + \frac{1}{2}\left(\frac{\epsilon a}{k}\right)^2[N_6 - \cos(2\zeta)] \tag{53}$$

where

$$N_6 = \frac{1}{2}(N_3 + N_4B + \tilde{N}_4\tilde{B}), \quad \zeta = kx - (\omega - \epsilon^2\psi_o)t$$

and

$$\psi_o = \frac{a^2}{4k^2}\beta$$

The term $(\omega - \epsilon^2\psi_o)$ represents the nonlinear dispersion relation where $\epsilon^2\psi_o$ is the nonlinear correction. Equation 53 is the Stokes wavetrain to second-order approximation.

STABILITY ANALYSIS

We have seen that time modulation can be regarded as a special case of general modulation process governed by the Schrodinger equation. This yielded the uniform Stokes wave train.

In a wave packet there are waves of different wavelengths. Usually the wave number is centered around a primary or predominant wave number. Therefore, in the derivation of the Schrodinger equation we assume that the wave packet can be represented by the primary wave number, while it is also implicitly assumed that $\delta k/k \ll 1$ where δk denotes the maximum variation in k within the wave packet. The instability occurs due to nonlinear interaction between the primary wave number and its sidebands. This phenomenon is known as resonance. Therefore, to simulate this sideband effect a small perturbation anlysis is done. Its details are given in Ahmed (1983) and in Hasimoto and Ono (1972).

It is a well-known result of this stability analysis that instability occurs when $\alpha\beta \geq 0$. Since α is always negative, the criterion for stability is given by $\beta \geq 0$. For $\beta < 0$ the system becomes unstable. The maximum amplication factor for unstable growth is given by

$$(A.F.)_{\max} = |\beta A_0^2| \tag{54}$$

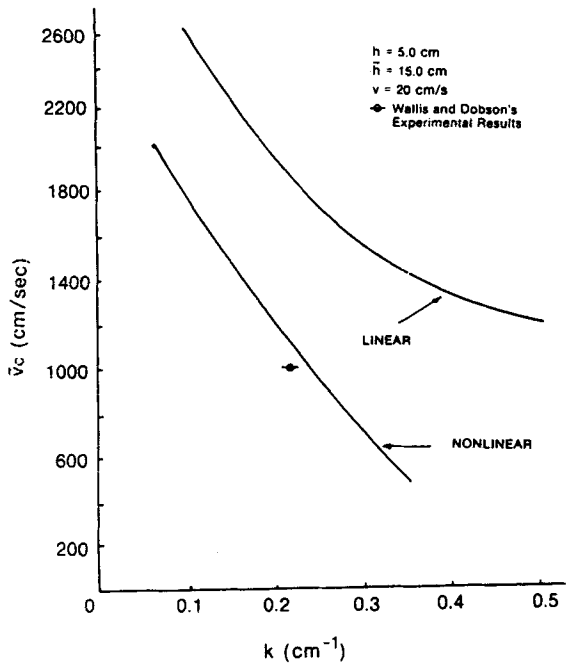

Figure 3. Comparisons of theoretical calculations with Wallis and Dobson's (1973) results. The uncertainty in the experimentally measured wavelengths is also shown.

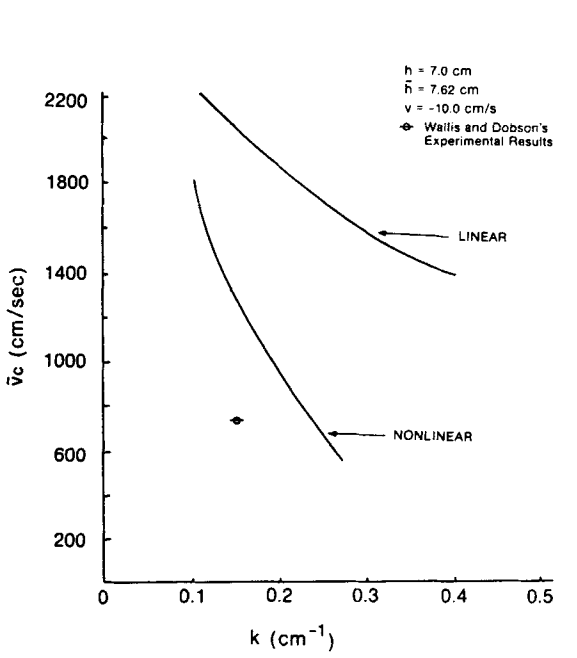

Figure 4. Comparisons of theoretical calculations with Wallis and Dobson's (1973) results. The uncertainty in the experimentally measured wavelengths is also shown.

for

$$\bar{k} = \left(\frac{\beta}{\alpha}\right)^{1/2} |dA_0|.$$

RESULTS

As discussed earlier, the nonlinear stability of the waves depends upon the signs of α and β, the two coefficients in the Schrodinger equation. Since α and β are very large and complicated functions of ρ', k, h, $\bar{h}$, v, and $\bar{v}$, a computer program was written to determine the sign of these coefficients for different flow parameters in an air-water system.

In most cases, initial (unperturbed) cocurrent and countercurrent velocities were given to water, and critical air velocities, $\bar{v}_c$, were determined for different values of k. It was found that $\bar{v}_c$ is very strongly dependent on k. Water depth, h, is also found to affect $\bar{v}_c$ to a considerable degree. For increasing k and h, the system tends to instability for fixed air velocity.

The critical air velocity, $\bar{v}_c$, has been plotted against the wave number k and is shown in Figures 3, 4, 5 and 6. The corresponding experimental results of Wallis and Dobson (1973) are also shown in the figures. It can be seen from the plots that nonlinear instability occurs at an air velocity which is far lower than the critical air velocity given by the linear analysis. This was also observed in the experiments. These theoretical predictions of critical air velocities from the nonlinear analysis are in much better agreement with the experimental data than the predictions of the linear analysis. Amplification factor was also plotted against air velocity and is shown in Figures 7 and 8. It is clear from these plots that the amplification factor of the unstable growth increases sharply with increasing air velocity. This is most clearly shown in curve *a*, Figure 8.

It appears that two different kind of instability mechanisms are at work. One is possible even in the absence of air velocity, and the wave train would just disintegrate due to this instability. The other, at high air velocity, may be responsible for the explosive growth of wave amplitude, which leads to the phase transition. This appears to be due to a Kelvin-Helmholtz type mechanism. This work

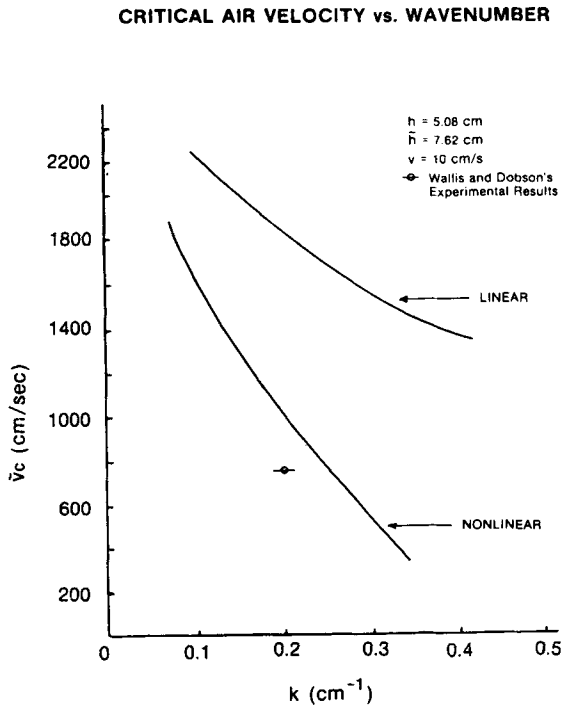

Figure 5. Comparisons of theoretical calculations with Wallis and Dobson's (1973) results. The uncertainty in the experimentally measured wavelengths is also shown.

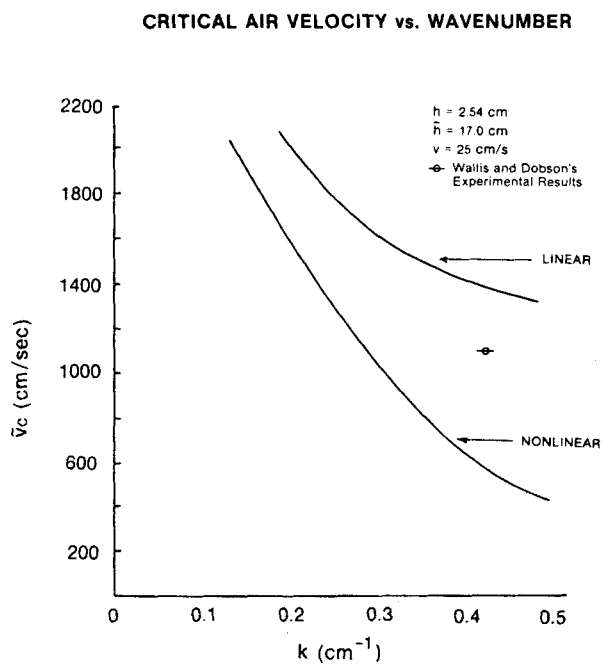

Figure 6. Comparisons of theoretical calculations with Wallis and Dobson's (1973) results. The uncertainty in the experimentally measured wavelengths is also shown.

therefore appears to explain why the transition to slug flow occurs at relative velocities well below that predicted for the linear Kelvin-Helmholtz instability. The effects of viscosity have been ignored with the implicit assumption that boundary layer effects are

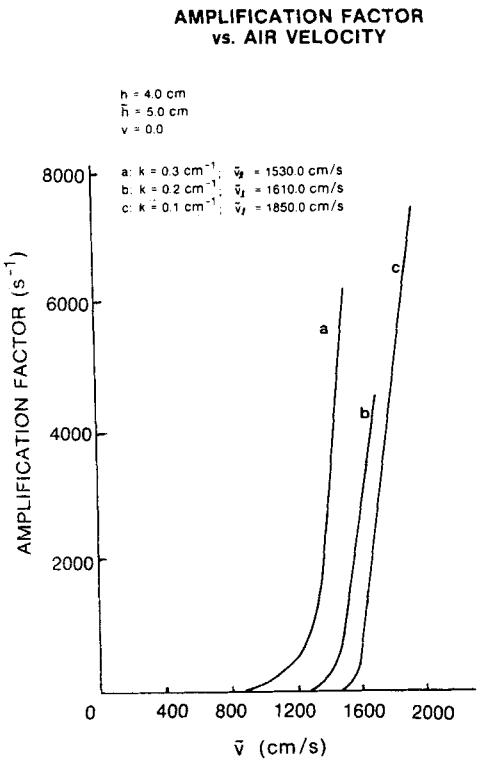

Figure 7. Amplification factors vs. air velocity for a 9 cm duct for various wavelengths. The linear instability limits ($\tilde{v}_l$) are tabulated in the figure.

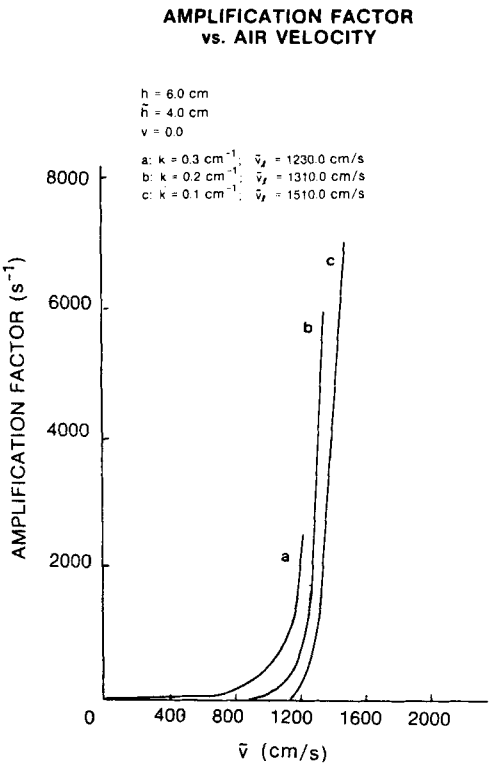

Figure 8. Amplification factors vs. air velocity for a 10 cm duct for various wavelengths. The linear instability limits ($\tilde{v}_l$) are tabulated in the figure.

confined to regions very close to the walls and the interface, and because the waves are long, they mainly affect the damping characteristics. However, a careful evaluation of viscous effects is desirable, though difficult, in future work.

ACKNOWLEDGMENT

We would like to thank the National Science Foundation for support of this work under Grant No. CP-81-12667.

NOTATION

G = $g(1-\rho')$
g = acceleration due to gravity
h = depth of channel occupied by lower fluid
$\tilde{h}$ = depth of channel occupied by upper fluid
i = $(-1)^{1/2}$
k = predominant wave number
p = $-i\dfrac{\partial}{\partial x}$
p_1 = $-i\dfrac{\partial}{\partial x_1}$
q = $i\dfrac{\partial}{\partial t}$
q_1 = $i\dfrac{\partial}{\partial t_1}$
q_2 = $i\dfrac{\partial}{\partial t_2}$
t = time

V = group velocity of the wave
v = the horizontal velocity of the lower fluid
$\tilde{v}$ = the horizontal velocity of the upper fluid
x = coordinate in the direction of flow
y = coordinate normal to the direction of flow

Greek Letters

η = elevation of the wave from the interface
ρ = density of the lower fluid
$\tilde{\rho}$ = density of the upper fluid
$\rho' = \frac{\tilde{\rho}}{\rho}$
Φ = total velocity potential of the lower fluid
$\tilde{\Phi}$ = total velocity potential of the upper fluid
φ = velocity potential of the lower fluid due to wave motion
$\tilde{\varphi}$ = velocity potential of the upper fluid due to wave motion
ϵ = small dimensionless parameter
ω = frequency of the wave
ϑ = phase of the wave
σ = $\tanh(kh)$
$\tilde{\sigma}$ = $\tanh(k\tilde{h})$
$\tilde{\sigma}_c$ = critical air velocity

LITERATURE CITED

Ahmed, R., "Finite Amplitude Wave Phenomena in Two-Phase Flow: Transition to Slug Flow," M.S. Thesis, Univ. of California, Santa Barbara (1983).

Benjamin, T. B., "Instability of Periodic Wave Trains in Nonlinear Dispersive Systems," *Proc. Roy. Soc.*, **A299**, 59 (1967).

Benjamin, T. B., and J. E. Feir, "The Disintergration of Wave Trains on Deep Water," *J. Fluid Mech.*, **27**, 417 (1967).

Hasimoto, H., and H. Ono, "Nonlinear Modulation of Gravity Waves," *J. Phy. Soc. Japan.*, **33**, 805 (1972).

Kordyban, E. S., and T. Ranov, "Mechanism of Slug Formation in Horizontal Two-Phase Flow," *J. Basic Eng.*, **92**, 857 (1970).

Lake, B. M., and H. C. Yuen, "Nonlinear Deep-Water Waves: Theory and Experiment, 2: Evolution of a Continuous Wave Train," *J. Fluid Mech.*, **83**, 49 (1977).

Nayfeh, A., *Perturbation Methods*, 228, Wiley-Interscience, New York (1973).

Stuart, J. T., and R. C. DiPrima, "The Eckhaus and Benjamin-Feir Resonance Mechanisms," *Proc. R. Soc. London*, **A362**, 27 (1978).

Taitel, Y., and A. E. Dukler, "A Model for Predicting Flow Regime Transitions in Horizontal and Near-Horizontal Gas-Liquid Flow, *AIChE J.*, **22**, 47 (1976).

Wallis, G. B., and J. E. Dobson, "The Onset of Slugging in Horizontal Stratified Air-Water Flow," *Int. J. Multiphase Flow*, **1**, 173 (1973).

Weissman, M. A., "Nonlinear Wave Packets in the Kelvin-Helmholz Instability," *Phil. Trans. Roy. Soc.*, **A290**, 639 (1978).

Whitham, G. B., "Nonlinear Dispersion of Water Waves," *J. Fluid, Mech.*, **27**, 399 (1967).

———, *Linear and Nonlinear Waves*, 586, Wiley-Interscience, New York (1974).

Manuscript received Jan. 30, 1984; revision received Oct. 16 and accepted Oct. 16, 1984.